

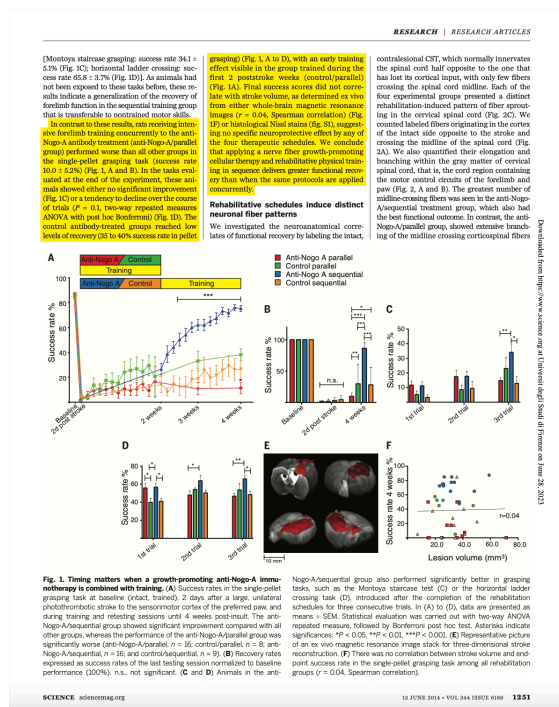
**PUBBLICAZIONE, AI SENSI DELL'ART. 19 DEL D.LGS N. 33 DEL 14 MARZO 2013, MODIFICATO DALL'ART. 18 DEL D.LGS N. 97 DEL 25 MAGGIO 2016 COME INTEGRATO DALL'ART.1 C. 145 DELLA LEGGE 27 DICEMBRE 2019 N. 160, DELLE DOMANDE DELLA PROVA COLLOQUIO STABILITE DALLA COMMISSIONE ESAMINATRICE DELLA SELEZIONE DI SEGUITO INDICATA NELLA RIUNIONE IN DATA 28/06/2023**

**BANDO N. 400.21 PNRR CNR-INO IR0006 IPHOQS CUP B53C22001750006**

Selezione per titoli e colloquio ai sensi dell'art. 8 del "Disciplinare concernente le assunzioni di personale con contratto di lavoro a tempo determinato", per l'assunzione, ai sensi dell'art. 83 del CCNL del Comparto "Istruzione e Ricerca" 2016-2018, sottoscritto in data 19 aprile 2018, di una unità di personale con profilo professionale di **Ricercatore III livello**, presso il CNR-Istituto Nazionale di Ottica, Sede di Sesto Fiorentino.

**BUSTA 1**

1. la candidata descriva un esperimento di imaging non lineare per lo studio della funzionalità corticale
2. la candidata faccia degli esempi, presi dalla letteratura, di utilizzo dell'imaging non lineare per studiare le lesioni del tessuto neuronale in vivo
3. la candidata legga e traduca il brano estratto dal seguente articolo: Wahl, Anna-Sophia, et al. "Asynchronous therapy restores motor control by rewiring of the rat corticospinal tract after stroke." *Science* 344.6189 (2014): 1250-1255.



**BUSTA 2 (estratta)**

1. La candidata descriva delle possibili applicazioni che prevedano l'utilizzo di microscopia non lineare per lo studio delle lesioni neuronali
2. La candidata descriva le componenti principali di un esperimento di microscopia non lineare in vivo.
3. La candidata legga e traduca il brano estratto dal seguente articolo: Wahl, Anna-Sophia, et al. "Asynchronous therapy restores motor control by rewiring of the rat corticospinal tract after stroke." *Science* 344.6189 (2014): 1250-1255.

**RESEARCH | RESEARCH ARTICLES**

(Fig. 2B) ( $P < 0.05$ , two-way repeated measures ANOVA with post hoc Bonferroni).

**A quantitative analysis of the distribution and density of ipsilaterally projecting corticospinal fibers using pattern-recognition algorithms to analyze both single corticospinal fibers and related fiber growth parameters (see supplementary materials and methods) confirmed overshooting fiber growth and aberrant termination patterns in the anti-Nogo-A/parallel group. In the anti-Nogo-A/sequential group, midline-crossing, sprouting corticospinal fibers displayed a medial organization with few branches and a preference for the premotor and motor spinal cord (laminae 6 to 9) (Fig. 2, D and G). In contrast, fibers in the anti-Nogo-A/parallel group appeared less organized with more than double the number of branches and a different laminar distribution including the dorsal, predominantly sensory laminae 1 to 5. We also assessed the connectivity of the ipsilaterally projecting corticospinal fibers by quantifying the density of axonal boutons recognized morphologically in the premotor interneuron, lamina 7. We detected a significantly higher bouton density in the anti-Nogo-A/parallel group compared with the anti-Nogo-A/sequential group (Fig. 2H) ( $P < 0.05$ , Student's *t* test, two-tailed, unpaired). The anti-Nogo-A/parallel group showed a greater tendency of axons to grow beyond the gray matter-white matter boundary, as well as a highly aberrant growth pattern (Fig. 2, I and 1). In the medio-ventral funiculus, such fibers are typically intermixed with sprouts of the small, unmyelinated ipsilateral CST.**

**Nerve cells from the intact forebrain cortex are responsible for recovery**

Our results suggest that the recovery of rat forelimb function after stroke in the anti-Nogo-A/sequential group originates from extensive and precise reinnervation of the stroke-densitized spinal hemisection by midline-crossing fibers from the intact motor cortex and CST. We tested this hypothesis in the animals of the anti-Nogo-A/sequential group, all of which showed excellent functional recovery, by using two different experimental approaches for (infectious, selective, and reversible) inactivation of the ipsilaterally projecting corticospinal fibers on the long and short term, respectively. For long-term blockade, we used a virus to deliver a doxycycline-inducible tetanus toxin to temporarily inactivate the synaptic release mechanism (5). We injected the highly efficient retrograde gene transfer lentiviral vector *H128* carrying enhanced tetanus neurotoxin light chain (*rtTnT*) with an enhanced green fluorescent protein (EGFP) downstream of a tetraacycline-responsive element (TRE) into the stroke-densitized side of the cervical spinal cord at level C5-C6, and we injected the adeno-associated serotype 2.1 (AAV2) vector carrying the reverse tetraacycline transactivator (rtTAV2, Tet-on) into the contralateral, intact premotor and motor cortex ( $n = 6$  animals) (Fig. 3, A and B). Only cortical neurons with axons projecting to the stroke-densitized spinal

**Fig. 2. Corticospinal tract sprouting depends on timing of rehabilitative training correlating with functional recovery.** The four rehabilitation schedules (anti-Nogo-A/parallel,  $n = 10$ ; control/parallel,  $n = 8$ ; anti-Nogo-A/sequential,  $n = 10$ ; and control/sequential,  $n = 8$ ) differently influenced the sprouting of corticospinal fibers from the intact side of the spinal cord across the spinal cord midline (M) (A) Low- and high-magnification micrographs of biotinylated dextran amine (BDA)-labeled corticospinal fibers in intact spinal hemisection (left) growing into the stroke-densitized hemisection (right; inset) at spinal cord level C4, D3 to D4. Lines for intersection counts with corticospinal fibers. Scale bar, 200  $\mu$ m. (B) Fibers crossing the midline (M) and branching in the gray matter at distances D1 to D4 were counted and normalized to the number of BDA-positive labeled fibers in the main tract. (C) Micrographs showing different sprouting patterns of corticospinal fibers from the ipsilateral cortex in the denervated cervical spinal cord (C4) in lamina 7 in the different treatment groups. Scale bars, 200  $\mu$ m. (D) Combining anti-Nogo-A immunoreactivity with simultaneous training (anti-Nogo-A/parallel) results in a significantly higher density of ipsilateral CST fibers in the stroke-densitized cervical spinal cord than does anti-Nogo-A/sequential treatment. (E) The most significant difference in fiber density between anti-Nogo-A/parallel and anti-Nogo-A/sequential animals was detected in lamina 6/7 and lamina 9 of the denervated cervical hemisection. Lamina 7 was also significant for increased fiber branching (F) (Branching index = branches per fiber per BDA-positive fibers in the intact CST) and bouton numbers (G) in the anti-Nogo-A/parallel group. (H and I) Significantly more fibers cross the gray matter-white matter boundaries in the dorsolateral (labeled with "A"), the ventrolateral (labeled "B"), and the ventro-medial funiculus (labeled "C" scheme shown in (H)) in the anti-Nogo-A/parallel group. Data are presented as means  $\pm$  SEM. Statistical evaluation was carried out with two-way ANOVA repeated measure, followed by Bonferroni post hoc (B) and Student's *t* test (two-tailed, unpaired) (D to G and I). Asterisks indicate significances: \*\* $P < 0.05$ , \*\*\* $P < 0.01$ , \*\*\*\* $P < 0.001$ .

1252 13 JUNE 2014 • VOL 344 ISSUE 6189 sciencemag.org SCIENCE

IL PRESIDENTE  
Prof. Leonardo Fallani



LA SEGRETARIA  
Dott.ssa Giulia Adembri

